Anisotropic Purcell Factor Control of an Emitter in Graphene Under the Modulation of a Static Magnetic Field

Zenghong Ma (zenghongma@mail.nankai.edu.cn)
Tianjin Sino-German University of Applied Sciences
Zijian Chen
Tianjin Sino-German University of Applied Sciences
Lian Zhang
Tianjin Sino-German University of Applied Sciences
Xiaocui Lu
Tianjin Sino-German University of Applied Sciences
Jian Xu
Tianjin Sino-German University of Applied Sciences
Guangwu Yang
Tianjin Sino-German University of Applied Sciences
Xin Xu
Tianjin Sino-German University of Applied Sciences

Research Article

Keywords: Anisotropic Purcell Factor , Emitter , Graphene, Static Magnetic Field

Posted Date: July 9th, 2021

DOI: https://doi.org/10.21203/rs.3.rs-691197/v1

Version of Record: A version of this preprint was published at Journal of the Optical Society of America B on January 3rd, 2022. See the published version at https://doi.org/10.1364/JOSAB.442888.

Anisotropic Purcell Factor Control of an Emitter in Graphene Under the Modulation of a Static Magnetic Field

Zenghong Ma[1,2,*], Zijian Chen[2,3], Lian Zhang[1,2], Xiaocui Lu[1], Jian Xu[4], Xin Xu[2,3], and Guangwu Yang[1]

[1]Basic Experimental and Training center, Tianjin Sino-German University of Applied Sciences, Tianjin, 300350, China
[2]Tianjin "the Belt and Road" Joint Laboratory(Research Center), Tianjin, 300350, China
[3]New Energy Department, Tianjin Sino-German University of Applied Sciences, Tianjin, 300350, China
[4]Basic Courses Department, Tianjin Sino-German University of Applied Sciences, Tianjin, 300350, China
[*]corresponding anthor: zenghongma@mail.nankai.edu.cn

ABSTRACT

Spontaneous emission control of emitters hold great promise for applications in photonics and quantum optics. As a definition of the spontaneous emission lifetime of an atom or molecule, the Purcell factor of an emitter coupled with graphene plasmons by a static magnetic field is studied. The results show that the Purcell factor can be effectively modulated by the applying of external magnetic field to graphene at lower terahertz frequencies. In addition, in the presence of a magnetic field, the coupling between the graphene and emitter becomes stronger, which results in a strong enhancement of the emission of the emitter and the numerically calculated Purcell factor is increased. More specifically, the Purcell factor increases by almost an order of magnitude when the applied magnetic field is 10T. Moreover, the Purcell factor also depends on the polarization direction of the emitter, especially when the polarization direction of the emitter is parallel to the graphene plane, the Purcell factor will show anisotropy with the change of polarization angle. Bias of the applied magnetic field extends a new path for the realization of Purcell factor modulation based on graphene-emitter interaction, it may provides a promising application value for the design of the photo-magnetic based quantum devices.

Introduction

Introduction

Since the first discovery of Purcell effect by E.M. Purcell in 1946, the Purcell factor (PF) was defined as the spontaneous emission lifetime of an atom or molecule, which depends both on the intrinsic properties of the emitter and on its interaction with environment[1]. The control of the interaction between a single emitter and matter has become a popular subject of research due to its potential application to quantum optics[2–5],light-emitting[6] and sensing[7,8]. A lot of research interests have been focused on the surrounding environment of an emitter to control the Purcell factor, including resonant cavities[9,10] and photonic crystals[11,12].

Due to their ability to suppress the electromagnetic field in subwavelength size to achieve local field enhancement, metal surface plasmons have been extensively studied in the past decades, the electromagnetic energy confinement make the strong coupling between emitters and surface plasmons possible, which can enormously modify the PF of a neighboring emitter[13–16]. However, plasmons support in metals are difficult to be modulate, which inevitably limit their application in plasmonic devices. Then, graphene has emerged as an alternative plasmonic material due to its extraordinary electronic and optical properties. Compared with metallic plasmons, graphene plasmons take more advantages in higher confinement and lower dissipation loss, which make graphene a promising material[17] for the emission control of emitters. The investigations focus on the interaction between emitters and surface plasmons in graphene have been made, such as in waveguides[18–20], or in ntennas[21–23]. In addition, the property of graphene can be easily modulated by electric doping[24],magnetostatic gating[25] or strain engineering[26]. By making full use of the highly tunable of graphene, the development of important applications in nanoplasmonics can be expected[27,28]. For example, in our previously reported work, we have shown that the spontaneous emission of emitters can be controlled by applying a strain engineering to graphene sheet. Under strain engineering, the graphene plasmons are anisotropic in-plane, which enables the anisotropy control of spontaneous emission of an emitter, such a mechanism is essential for the design of strain sensors and quantum devices[29]. Apart from the electronic or mechanical tunability, the properties of graphene

can be dynamically tuned through magnetostatic bias, which is another major feature of graphene[30–32]. It has been reported that when applying an external magnetic field perpendicular to graphene sheet, a hybridization occurs between the cyclotron excitation and the plasmon, resulting in a magneto-plasmon mode[33,34]. Lots of reports have focused on the manipulation of Faraday rotation in graphene, which represents the property of dichroism under a magnetic bias[35–38].However, the use of external magnetic fields to control the spontaneous emission of emitters coupled to magneto-plasmon mode in graphene has been rarely studied.

In this paper, we propose a new mechanism to actively tune the PF of a THz emitter coupled with the magneto-plasmon modes in a graphene sheet .We show that magnetic field B can effectively control the emission of the emitter. For emitters whose polarization direction is perpendicular to graphene, the PF of the emitter will enhance by an order of magnitude with the application of magnetic field. Besides, azimuthal angle dependent of PF for the emitter's polarization direction parallel to the sheet can be seen in the paper. Here the Purcell factor show anisotropic as the change of the azimuthal angle α, it traced back to the anisotropic conductivity of graphene bias by a magnetic field. Modulation of emitter spontaneous emission by external magnetic field can be integrated into the design of magneto-plasmon based quantum devices to further expand its application.

Materials and Methods

The conductivities of graphene under a static magnetic field

Figure 1 depicts the configuration in our study. a static magnetic was perpendicular applied to a single layer graphene. Considering the graphene sheet is placed on the x-y plane in cartesian coordinates, and the biased magnetic field is along the z-axis, the conductivity can be written as the following tensorial form[39]

$$\widetilde{\sigma} = \begin{pmatrix} \sigma_{xx} & \sigma_{xy} \\ \sigma_{yx} & \sigma_{yy} \end{pmatrix} \tag{1}$$

The diagonal and non-diagonal element of the conductivity tensor represent the Longitudinal and Hall conductivities respectively. The expression should contain all allowed conversions between the Landau levels[34].However, the conductivity can be simplified to the classical Drude formula for highly doped graphene[40]

$$\sigma_{xx} = \sigma_{yy} = \sigma(\omega)\frac{1+i\omega\tau}{(1+i\omega\tau)^2+(\omega_c\tau)^2} \tag{2}$$

$$\sigma_{xy} = -\sigma_{yx} = \sigma(\omega)\frac{\omega_c\tau}{(1+i\omega\tau)^2+(\omega_c\tau)^2} \tag{3}$$

where $\tau = \mu\mu_c/ev_F^2$ is a relaxation time, $\omega_c = eBv_F^2/\mu_c$ is the cyclotron frequency, μ is the carrier mobility, μ_c is the chemical potential and $v_F \approx c/300$ represent the Fermi velocity. The $\sigma(\omega)$ represent the static optical conductivity of single graphene in absence of magnetic field, by using the local-random phase approximation (RPA), the isotropic conductivity of graphene can be expressed as[41]

$$\sigma(\omega) = \frac{2e^2\tau k_B T}{\pi\hbar^2} ln[2cosh\frac{\mu_c}{2k_B T}] \tag{4}$$

In the following simulations, the chemical potential is taken as μ_c=0.4eV, the carrier mobility is $\mu = 10000\ \mathrm{cm}^2/\mathrm{Vs}$ and the temperature is T=300 K.

The analytical calculation method of the PF for anisotropic flat plate structure

According to Poynting's theorem, the rate of energy dissipation P=dW/dt read as[42]

$$\mathbf{P} = \frac{d\mathbf{W}}{dt} = \frac{2}{\hbar}\mathrm{Im}\{\mathbf{p}^* \cdot \mathbf{E}(r_0)\} \tag{5}$$

Where **p*** is the momentum of an dipole emitter, $\mathbf{E}(r_0)$ is the electric filed at the emitter's origin r_0. Consider an emitter placed in an inhomogeneous environment, the filed $\mathbf{E}(r_0)$ consists the primary electric field $\mathbf{E}_0(r_0)$ and the induced field $\mathbf{E}_s(r_0)$, i.e. $\mathbf{E}(r_0)$= $\mathbf{E}_0(r_0)$+$\mathbf{E}_s(r_0)$. Then, the total rate of energy dissipation P can be split into two parts

$$\mathbf{P} = \mathbf{P}_0 + \frac{2}{\hbar}\mathrm{Im}\{\mathbf{p}^* \cdot \mathbf{E}_s(r_0)\} \tag{6}$$

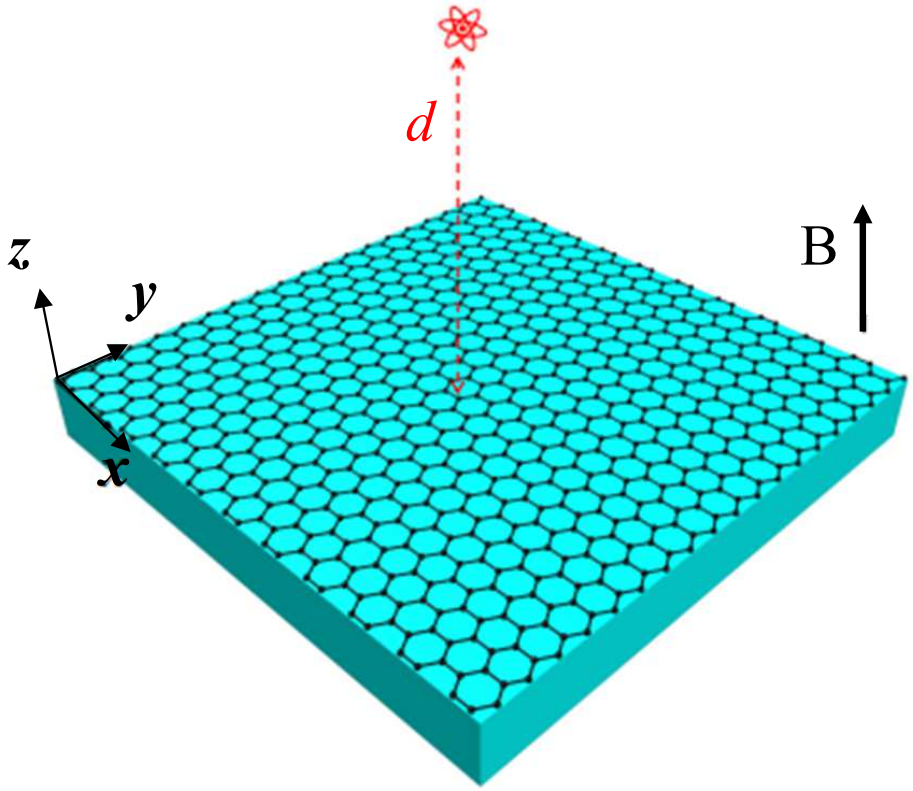

Figure 1. Schematics of an optical emitter located several nanometers above an infinite graphene sheet. An external static magnetic field is applied vertically to the graphene sheet, and its direction is along the positive direction of the z-axis.

where $\mathbf{P}_0 = 4k_0^3|\mathbf{p}|^2/3\hbar$ is the free-space spontaneous emission rate. Thus, by calculating the induced filed $\mathbf{E}_s(r_0)$ at the emitter's origin r_0, one can get the total energy emission of an emitter. When an emitter placed near a planar interfaces, the spontaneous emission rate can be analytical calculated by the decomposition of the dyadic Green's function, using the angular spectrum representation, the dyadic Green's function can be identified as an integral form.

To be specific, consider an emitter placed above a graphene sheet, the spontaneous emission rate for the emitter polarized perpendicular to the graphene sheet reads as

$$\mathbf{P} = \mathbf{P}_0 + \frac{1}{2\pi\hbar}\int_0^\infty\int_0^{2\pi} k_\parallel dk_\parallel d\varphi \mathrm{Re}\{2|p_z|^2 {k_\parallel}^2 r_p(\varphi)\frac{e^{2ik_\perp d}}{k_\perp}\}, \tag{7}$$

when the polarization of the emitter is in-plane, we obtain

$$\begin{aligned}\mathbf{P} = \mathbf{P}_0 + \frac{1}{\pi\hbar}\int_0^\infty\int_0^{2\pi} k_\parallel dk_\parallel d\varphi \mathrm{Re}\{|p_x\sin\varphi - p_y\cos\varphi|^2 \times \\ (k_0{}^2 r_s(\varphi) - {k_\perp}^2 r_p(\varphi))\frac{e^{2ik_\perp d}}{k_\perp}\}.\end{aligned} \tag{8}$$

where $p_x = p\sin\alpha, p_y = p\cos\alpha$, α is the polarization angle of emitter in-plane.

where r_p and r_s are the Fresnel reflection coefficients have the form of[22]

$$\begin{aligned} r_p &= \frac{\varepsilon k_\perp - k_\perp^{'} + 4\pi\sigma_c k_\perp k_\perp^{'}/\omega}{\varepsilon k_\perp + k_\perp^{'} + 4\pi\sigma_c k_\perp k_\perp^{'}/\omega}, \\ r_s &= \frac{k_\perp - k_\perp^{'} - 4\pi\sigma_c k_0/c}{k_\perp + k_\perp^{'} + 4\pi\sigma_c k_0/c}, \end{aligned} \tag{9}$$

Here ε is the permittivity of the backing material, the light wave vector in vacuum is $k_0 = \omega/c$, $k_\parallel$ is the transverse wavenumber, $k_\perp = \sqrt{k_0^2 - k_\parallel^2}$ and $k'_\perp = \sqrt{\varepsilon k_0^2 - k_\parallel^2}$ are the longitudinal wavenumber in the upper and lower half space and z_0 is the distance between the emitter and graphene sheet. Under the magnetic filed bias, the conductivity of graphene shows anisotropic, then the anisotropic conductivity can be represented as $\sigma_c(\omega) = \sigma_{xx}(\omega)\cos^2\varphi + \sigma_{yy}(\omega)\sin^2\varphi$ under the polar coordinate system. By the definition of PF, the PF of the system can be calculated as

$$PF = \mathbf{P}/\mathbf{P}_0 \tag{10}$$

introducing Eq.(7)-Eq.(9) into the last equation, one can get the PF of an emitter placed near the infinite graphene control by an external magnetic field.

Results

The Longitudinal and Hall conductivities

First of all, the diagonal element σ_{xx} and non-diagonal element σ_{xy} of the conductivity tensor were calculated according Eq.(2) and (3), which represent the Longitudinal and Hall conductivities respectively. First of all, the diagonal element σ_{xx} and non-diagonal element σ_{xy} of the conductivity tensor were calculated according Eq.(2) and (3), which represent the Longitudinal and Hall conductivities respectively. Figures 2(a) and (b) shows the real and imaginary part of the Longitudinal conductivity for the case of the graphene biased by a static magnetic field of B=2 T (blue line), 5 T (red line), 8 T (green line) and 10 T (purple line) respectively. At the meantime, the conductivity of the graphene for the case of B=0 T (the black line) was calculated for comparison. One can find that with the increase of the external magnetic field, the Longitudinal conductivity spectrum redshifted. Moreover, the value of the conductivity decreases significantly after the magnetic field is applied, because part of the conductivity contributes to Hall conductivity. Then, how the Hall conductivityσ_{xy} changes was also depicted in Figs.2 (c) and (d). Here the real and imaginary parts of the Hall conductivity are also redshifted. And we found that at high frequencies, the longitudinal conductivity values tend to be the same as those in the absence of a magnetic field, meanwhile, the value of Halls conductivity tends to zero. This means that the applied of the magnetic field has no effect on the change of conductivity at high frequencies, which can be traced back to the Eqs.(2)and (3) only consider the intra-band transitions.

PF control in magnetic biased graphene

We start with a vertically polarized emitter on top of the graphene, in the calculations below, suspended graphene is taken into account. Figure 3 shows how the of PF of the emitter changes when different magnetic fields B are applied to graphene. Firstly, when no magnetic field is applied to graphene, the PF was calculated for B=0 T, as the black line shown in Fig.3(a). It can be found that the PF value decreases with the increase of transmission frequency. In addition, compared with the spontaneous emission in vacuum, the spontaneous emission in the graphene environment can be increased by more than 6 orders of magnitude in the low-frequency region. This huge enhancement comes from the high confinement of the plasmon supported by graphene and the presence of large optical local density states in the vicinity of graphene. Then consider applying a static magnetic field perpendicular to the graphene sheet with a magnetic field intensity B. The blue, red, green and purple line in Fig.3(a) represent for the case of B= 2 T, 5 T, 8 T and 10 T, respectively. By comparison, it can be found that the trend of the curves remains the same after the application of magnetic field to graphene, but at low frequencies, the value of PF increases several times compared to the case without magnetic field. But at higher frequencies, the PF curves with and without the magnetic field almost coincide. Since the excitation of graphene plasmons at low frequencies contributes mainly to the enhancement of PF[22], this implies that the control of PF by magnetic fields is mainly from the modulation of graphene plasmons excited in graphene by a static magnetic field at low frequencies. Besides, how the PF value changes with respect to magnetic field B was calculated in Fig.3(b), comparisons are being drawn between the incidence frequencies of 1THz (black line) and 3THz (blue line). Therefore, we can conclude that the PF can be controlled in the low frequency by the applied magnetic field.

After studying the radiation of the vertically polarized emitter, we also calculated the PF of the emitter with the polarized direction parallel to the graphene surface. Here, the in-plane azimuthal angle between the polarization direction of the emitter and the x-axis is assumed to be α. When a magnetic field of intensity of 5T is applied to graphene, we calculate the changes in the PF of the emitter with different azimuth angle α, as shown in Fig.4(a). First, the blue and green lines represent the emission when the emitter's polarization direction is along (i.e. $\alpha = 0^\circ$) or perpendicular (i.e. $\alpha = 90^\circ$)to the x-axis, respectively. Then, The PF for the case of the azimuthal angles $\alpha = 45^\circ$(red line),135°(purple circle) and 180° (cyan circle) are calculated through analytic computation. Besides, the PF for the graphene in absence of magnetic field were calculated for the convenience of comparison, as shown by the black line in the figure. The value of the PF decreases with the increase of the emitter frequency, and the curves are trending in the same way compare to the case of B=0 T (black line), until the PF curve was almost coincided at higher frequencies. And the calculation results show that the control of PF by the external magnetic field is anisotropic in-plane, and it changes periodically with the azimuthal angle α. Then, how the PF changes with the angle α when the optical

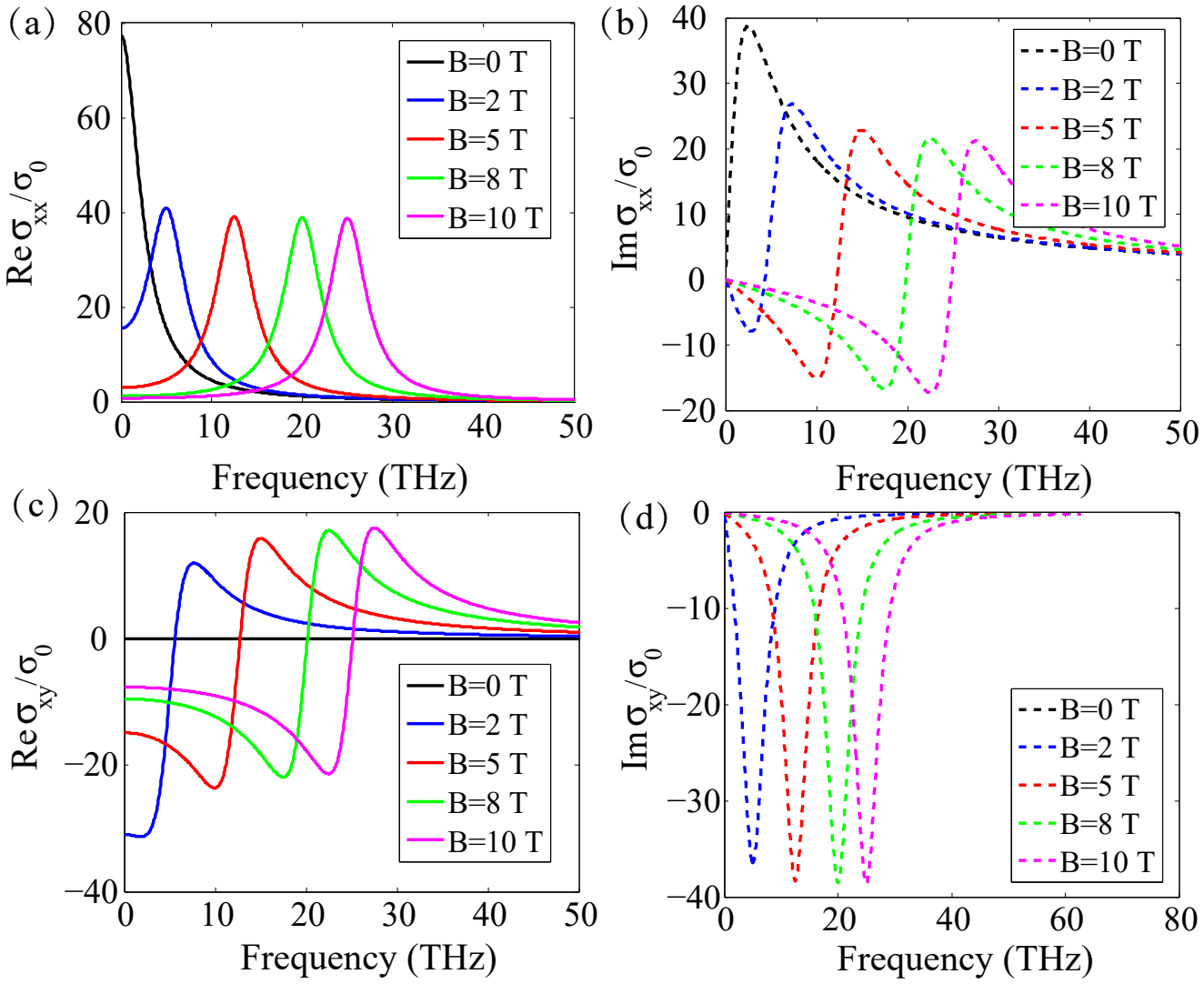

Figure 2. The anisotropic optical conductivity of graphene under a static magnetic field, The real (a) and imaginary part (b) of the diagonal conductivity σ_{xx} considering different magnetic intensity B. The real (c) and imaginary part (d) of the Hall conductivity σ_{xy} for various magnetic intensity B. The diagonal and Hall conductivities normalized to $\sigma_0 = e^2/\hbar$.

emitter at the frequency of 1THz is depict in Figure 4(b). The situations with the case of B=2 T (blue line), 5 T (red line), 8 T (green line) and 10 T (purple line) were calculated to compare with the case of B=0 (black line). It can be seen that the PF varies periodically with α, which is due to the in-plane anisotropy of the conductivity of graphene in the magnetic field. Moreover, it can be found that when the emitter is polarized along the $x$axis, the value of PF reaches the maximum, and when the emitter's polarization direction is perpendicular to the x axis, the value of PF reaches the minimum. In other words, the spontaneous emission for the emitter with different polarization direction can also be controlled by tuning the applied magnetic field.

To better describe the PF controlled by magnetic field, Fig. 5 plot the difference in the PF relative to the case of B =0 T. By comparing the emitter above the graphene with and without magnetic field bias, we can define Δ_{PF}=$(PF_B - PF_0)/PF_0 \times 100\%$ as the relative difference of PF. First of al, Δ_{PF} depends on the photon frequency and magnetic intensity B for a vertically polarized emitter is shown in Fig. 5(a). It can be found that at lower frequency, with the increase of the magnetic intensity B, the Δ_{PF} increase gradually, and the maximum of Δ_{PF} is close to about 1000% for B=10 T. Next, we consider an emitter with a photon frequency of 1 THz whose polarized direction is along the graphene sheet. Figure 5(b) depicts PF determined by the in-plane polarization angle α and magnetic intensity B. In accordance with the Fig. 4(b), for different angles α, Δ_{PF} is anisotropic and changes periodically. In addition, with the decrease of magnetic intensity B, the value of PF tends to be isotropic. It is worth mentioning that when the emitter's polarization direction is along the $x$axis, Δ_{PF}can reach 1000%. It can be seen that the anisotropic radiation of the emitter whose polarization direction is in the plane can be effectively controlled by

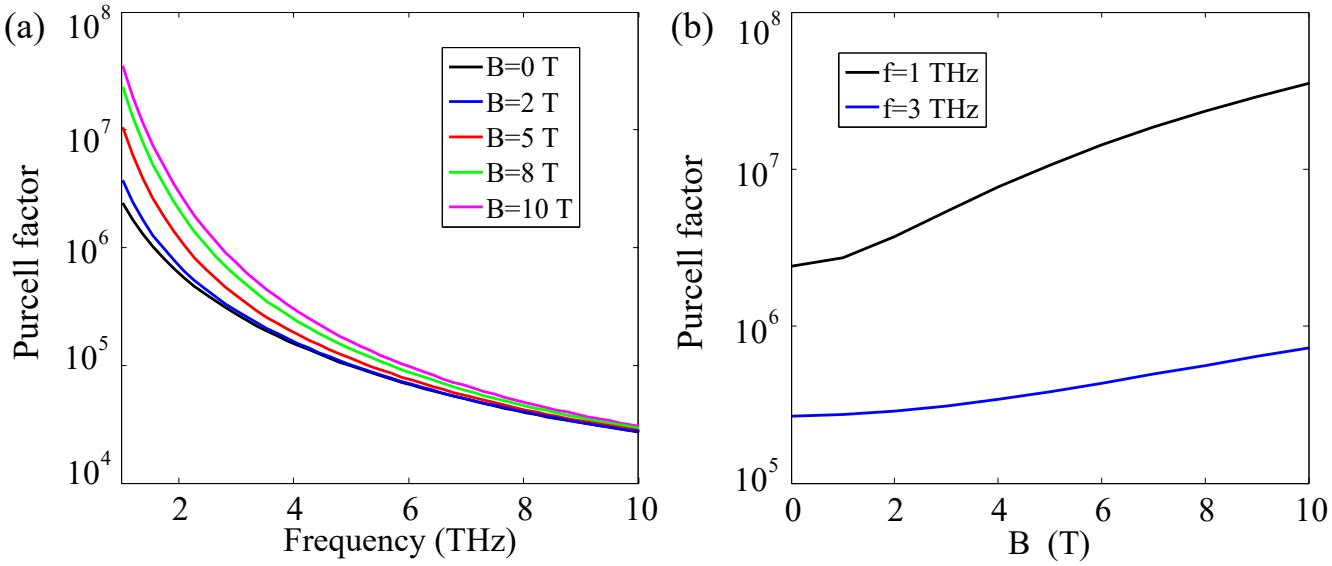

Figure 3. The PF of a vertically polarized emitter located 10 nm above the graphene sheet (a) The PF are plotted for various values of the applied magnetic field B. (b) The PF as a function of the magnetic field B with the incidence frequencies of 1THz (black line) and 3THz (blue line).

adjusting the external magnetic field.

Next, on account of that the PF depends strongly on the distance of the optical emitter placed. The distance dependence of PF for graphene sheet under magnetic field of B=2 T (blue line), 5 T (red line), 8 T (green line) and 10 T (purple line) or in absence of magnetic B=0 (black line) were calculated in Fig. 6, and the photon frequency is 1THz. It can be found that the value of PF decreases with the increase of distance d, with or without considering an external magnetic field. That is to say, the variation of distance has no effect on the value of PF controlled by the biased magnetic field.

Conclusions

In summary, the anisotropic response of graphene when a perpendicular magneto-static applied to graphene sheet in THz range were investigated in the paper, proving that the external magnetic bias can modulate the optical local density of states of graphene and thus control the PF of the emitter in it. To be more specific, the surface plasmon mode supported by graphene can achieve field enhancement to enhance the PF, on the one hand, when an external magnetic field is applied to graphene, the PF of the emitter can be further enhanced. On the other hand, when the magnetic field is strong enough, such as 10T, the PF can be enhanced by 1000%. In addition, anisotropy PF of the emitter can be achieved when the emitter oscillates in the direction along the graphene sheet.This develops a new approach for controlling the interaction of light and matter, which is expected to be further applied in the fields of optical constraint and topological transition, integrated optics and quantum devices.

References

1. Purcell, E. M., Torrey, H. C. & Pound, R. V. Resonance absorption by nuclear magnetic moments in a solid. *Phys. Rev.* **69**, 37–38 (1946).
2. Noda, S., Fujita, M. & Asano, T. Spontaneous-emission control by photonic crystals and nanocavities. *Nat. Photon.* **1**, 449–458 (2007).
3. Akimov, A. V. *et al.* Generation of single optical plasmons in metallic nanowires coupled to quantum dots. *Nature* **450**, 402–6, DOI: 10.1038/nature06230 (2007).
4. Laucht, A. *et al.* Electrical control of spontaneous emission and strong coupling for a single quantum dot. *New J. Phys.* **11**, 023034 (2009).
5. Galfsky, T. *et al.* Broadband enhancement of spontaneous emission in two-dimensional semiconductors using photonic hypercrystals. *Nano Lett.* **16**, 4940–4945, DOI: 10.1021/acs.nanolett.6b01558 (2016).
6. Santori, C., Pelton, M., Solomon, G., Dale, Y. & Yamamoto, Y. Triggered single photons from a quantum dot. *Phys. Rev. Lett.* **86**, 1502–1505, DOI: 10.1103/PhysRevLett.86.1502 (2001).

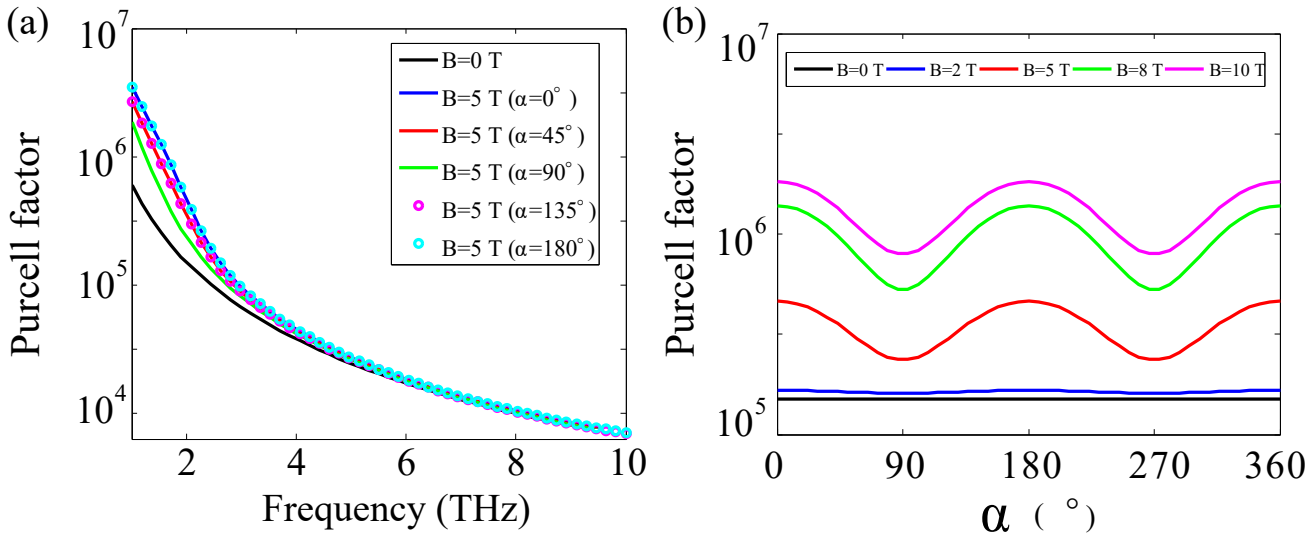

Figure 4. The analytically calculated PF of the emitter whose polarization direction is along the graphene plane. (a)The PF are plotted for the azimuthal angle $\alpha = 0°$(blue line), 45°(red line),90°(green),135°(purple circle) and 180° (cyan circle) when the applied magnetic field B=5T, compared to the PF for the case of B=0T (black line). (b)The variation of PF with different polarization directions in the plane α, where the frequency of the emitter is 1THz and the applied magnetic field intensity were 0, 2, 5, 8,10T respectively.

7. Moskovits, M. Surface-enhanced spectroscopy. *Rev. Mod. Phys.* **57**, 783–826 (1985).

8. Kundu, J., Le, F., Nordlander, P. & Halas, N. J. Surface enhanced infrared absorption (seira) spectroscopy on nanoshell aggregate substrates. *Chem. Phys. Lett.* **452**, 115–119 (2008).

9. Gerard, J. M. *et al.* Enhanced spontaneous emission by quantum boxes in a monolithic optical microcavity. *Phys. Rev. Lett.* **81**, 1110–1113 (1998).

10. Birnbaum, K. M. *et al.* Photon blockade in an optical cavity with one trapped atom. *Nature* **436**, 87–90, DOI: http://www.nature.com/nature/journal/v436/n7047/suppinfo/nature03804_S1.html (2005).

11. Lodahl, P. *et al.* Controlling the dynamics of spontaneous emission from quantum dots by photonic crystals. *Nature* **430**, 654–657 (2004).

12. Englund, D. *et al.* Controlling the spontaneous emission rate of single quantum dots in a two-dimensional photonic crystal. *Phys. Rev. Lett.* **95**, 013904 (2005).

13. Chang, D. E., Sorensen, A. S., Hemmer, P. R. & Lukin, M. D. Quantum optics with surface plasmons. *Phys. Rev. Lett.* **97**, 053002, DOI: 10.1103/PhysRevLett.97.053002 (2006).

14. Archambault, A. *et al.* Quantum theory of spontaneous and stimulated emission of surface plasmons. *Phys. Rev. B* **82**, 035411 (2010).

15. Qin, J., Liu, Y., Luo, H., Jiang, Z. & Wang, L. Tunable light emission by electrically excited plasmonic antenna. *ACS Photonics* **6**, 2392–2396 (2019).

16. Tobing, L., Birowosuto, D., Fong, K. E., Gao, Y. & Zhang, D. H. Plasmon–exciton systems with high quantum yield using deterministic aluminium nanostructures with rotational symmetries. *Nanoscale* **11** (2019).

17. Geim, A. K. & Novoselov, K. S. The rise of graphene. *Nat. Mater.* **6**, 183–191 (2007).

18. Kort-Kamp, W. J. M. *et al.* Active magneto-optical control of spontaneous emission in graphene. *Phys. Rev. B* **92**, 205415 (2015).

19. Tielrooij, K. J. *et al.* Electrical control of optical emitter relaxation pathways enabled by graphene. *Nat. Phys.* **11**, 281–287, DOI: 10.1038/Nphys3204 (2015).

20. Cuevas, M. Surface plasmon enhancement of spontaneous emission in graphene waveguides. *J. Opt.* **18**, 105003 (2016).

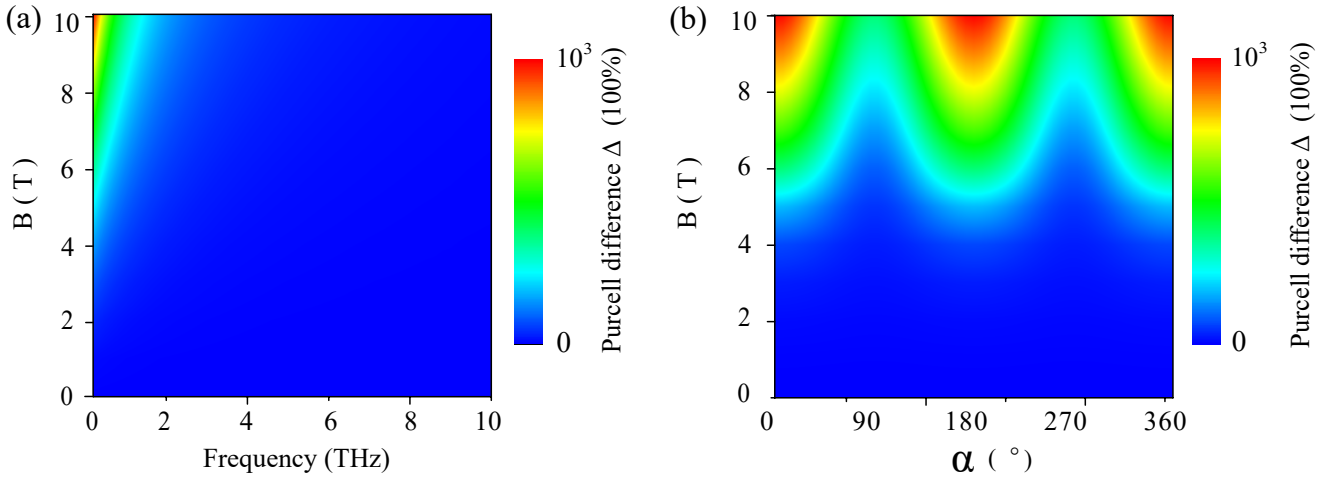

Figure 5. (a)The PF difference Δ_{PF} of a vertically polarized emitter relied on Frequency and magnetic intensity B. (b) The PF difference Δ_{PF} of a in-plane polarized emitter determined by the azimuthal angle α and magnetic intensity B.

21. Zhang, L., Fu, X., Zhang, M. & Yang, J. Spontaneous emission in paired graphene plasmonic waveguide structures. *Opt. Express* **21**, 7897–7907 (2013).

22. Koppens, F. H., Chang, D. E. & Garcia de Abajo, F. J. Graphene plasmonics: a platform for strong light-matter interactions. *Nano Lett.* **11**, 3370–7, DOI: 10.1021/nl201771h (2011).

23. Cuevas, M. Theoretical investigation of the spontaneous emission on graphene plasmonic antenna in thz regime. *Superlattices Microstruct.* **122**, 216–227, DOI: https://doi.org/10.1016/j.spmi.2018.08.006 (2018).

24. Wang, L. *et al.* Mid-infrared plasmon induced transparency in heterogeneous graphene ribbon pairs. *Opt. Express* **22**, 32450–32456, DOI: 10.1364/OE.22.032450 (2014).

25. Wu, J.-Y., Chen, S.-C., Roslyak, O., Gumbs, G. & Lin, M.-F. Plasma excitations in graphene: Their spectral intensity and temperature dependence in magnetic field. *ACS nano* **5**, 1026–1032 (2011).

26. Ni, Z. H. *et al.* Uniaxial strain on graphene: Raman spectroscopy study and band-gap opening. *ACS Nano* **2**, 2301–2305, DOI: 10.1021/nn800459e (2008).

27. Wei, H. *et al.* Polarization dependence of surface-enhanced raman scattering in gold nanoparticle- nanowire systems. *Nano letters* **8**, 2497–2502 (2008).

28. Akselrod, G. M. *et al.* Probing the mechanisms of large purcell enhancement in plasmonic nanoantennas. *Nat. Photonics* **8**, 835–840 (2014).

29. Ma, Z. *et al.* Dynamic spontaneous emission control of an optical emitter coupled to plasmons in strained graphene. *Opt. express* **25**, 23070–23081 (2017).

30. Goerbig, M. O. Electronic properties of graphene in a strong magnetic field. *Rev. Mod. Phys.* **83**, 1193–1243, DOI: 10.1103/RevModPhys.83.1193 (2011).

31. Goerbig, M. O., Moessner, R. & Douçot, B. Electron interactions in graphene in a strong magnetic field. *Phys. Rev. B* **74**, 161407 (2006).

32. Ferreira, A., Peres, N. M. R. & Castro Neto, A. H. Confined magneto-optical waves in graphene. *Phys. Rev. B* **85**, 205426, DOI: 10.1103/PhysRevB.85.205426 (2012).

33. Gusynin, V. P., Sharapov, S. G. & Carbotte, J. P. Magneto-optical conductivity in graphene. *J. Physics: Condens. Matter* **19**, 026222, DOI: 10.1088/0953-8984/19/2/026222 (2006).

34. Gusynin, V. P. & Sharapov, S. G. Transport of dirac quasiparticles in graphene: Hall and optical conductivities. *Phys. Rev. B* **73**, 245411, DOI: 10.1103/PhysRevB.73.245411 (2006).

35. I. *et al.* Intrinsic terahertz plasmons and magnetoplasmons in large scale monolayer graphene. *Nano Lett.* **12**, 2470–2474 (2012).

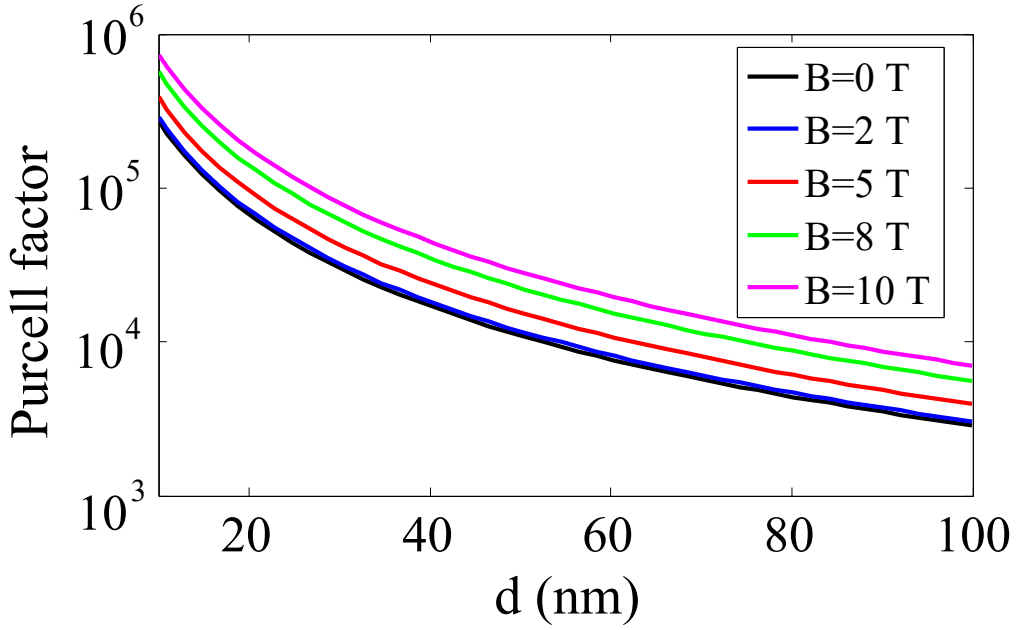

Figure 6. Distance dependence of the PF with different magnetic intensities B for the photon frequency of 1THz.

36. Tymchenko, M., Nikitin, A. Y. & Martín-Moreno, L. Faraday rotation due to excitation of magnetoplasmons in graphene microribbons. *Acs Nano* **7**, 9780–7 (2013).

37. Liu, J. Q., Wu, S., Zhou, Y. X. & Zayats, A. Giant faraday rotation in graphene metamolecules due to plasmonic coupling. *J. Light. Technol.* 1–1 (2018).

38. Dolatabady, A. & Granpayeh, N. Manipulation of the faraday rotation by graphene metasurfaces. *J. Magn. & Magn. Mater.* **469**, 231–235 (2019).

39. Hanson, G. W. Dyadic green's functions for an anisotropic, non-local model of biased graphene. *IEEE Transactions on Antennas Propag.* **56**, 747–757, DOI: 10.1109/TAP.2008.917005 (2008).

40. Gusynin, V. P., Sharapov, S. G. & Carbotte, J. P. On the universal ac optical background in graphene. *New J. Phys.* **11**, 095013, DOI: 10.1088/1367-2630/11/9/095013 (2009).

41. Wunsch, B., Stauber, T., Sols, F. & Guinea, F. Dynamical polarization of graphene at finite doping. *New J. Phys.* **8**, 318 (2006).

42. Novotny, L. & Hecht, B. *Principles of nano-optics* (Cambridge University, 2012).

Acknowledgements

This work was financially supported by the Tianjin Technical Expert Project under grant(20YDTPJC01770); Research Project of Tianjin Municipal Education Commission(2020KJ088); The Science and Technology Development Fund of Tianjin Education Commission for Higher Education (2020ZD03); University-level research project of TianjinSino-German University of Applied Sciences under grants (zdkt2017-001, zdkt2018-001). The authors acknowledge help from their institutions and much support from TEDA Applied Physics Institute of Nankai University(Tianjin).

Authour Contributions

Z.M.initiated the idea and built the model. Z.C., L.Z., X.L., J.X., X.X. and G.Y. performed analysis. All authors contributed to the scientific discussion and revision of the article.

additional information

Competing financial interests: The authors declare no competing financial interests.